In Proc SPIE, Vol. 6512,
Medical Imaging,
65122J-1-65122J-11

Subcortical Structure Segmentation using Probabilistic Atlas Priors

Sylvain Gouttard[a], Martin Styner[a,b], Sarang Joshi[c], Rachel G. Smith[a], Heather Cody[a], Guido Gerig[a,b]

[a]Department of Psychiatry, University of North Carolina, Chapel Hill NC, USA;
[b]Department of Computer Science, University of North Carolina, Chapel Hill NC, USA
[c]Deptartment of Biomedical Engineering, University of Utah, Salt Lake City, Utah, USA

ABSTRACT

The segmentation of the subcortical structures of the brain is required for many forms of quantitative neuroanatomic analysis. The volumetric and shape parameters of structures such as lateral ventricles, putamen, caudate, hippocampus, pallidus and amygdala are employed to characterize a disease or its evolution. This paper presents a fully automatic segmentation of these structures via a non-rigid registration of a probabilistic atlas prior and alongside a comprehensive validation.

Our approach is based on an unbiased diffeomorphic atlas with probabilistic spatial priors built from a training set of MR images with corresponding manual segmentations. The atlas building computes an average image along with transformation fields mapping each training case to the average image. These transformation fields are applied to the manually segmented structures of each case in order to obtain a probabilistic map on the atlas. When applying the atlas for automatic structural segmentation, an MR image is first intensity inhomogeneity corrected, skull stripped and intensity calibrated to the atlas. Then the atlas image is registered to the image using an affine followed by a deformable registration matching the gray level intensity. Finally, the registration transformation is applied to the probabilistic maps of each structures, which are then thresholded at 0.5 probability.

Using manual segmentations for comparison, measures of volumetric differences show high correlation with our results. Furthermore, the dice coefficient, which quantifies the volumetric overlap, is higher than 62% for all structures and is close to 80% for basal ganglia. The intraclass correlation coefficient computed on these same datasets shows a good inter-method correlation of the volumetric measurements. Using a dataset of a single patient scanned 10 times on 5 different scanners, reliability is shown with a coefficient of variance of less than 2 percents over the whole dataset. Overall, these validation and reliability studies show that our method accurately and reliably segments almost all structures. Only the hippocampus and amygdala segmentations exhibit relative low correlation with the manual segmentation in at least one of the validation studies, whereas they still show appropriate dice overlap coefficients.

Keywords: Segmentation, Shape, Shape analysis, Validation

1. INTRODUCTION

Magnetic resonance imaging (MRI) is able to provide a detailed information of normal and diseased anatomy for medical research and has become a significant imaging modality in clinical diagnosis and brain studies. Segmentation of subcortical structures from MR brain scans is a critical task that has many applications such as volume assessments and shape analysis. Segmenting structures is also necessary in various type of clinical studies assessing morphological changes correlated with medical treatments. Even though manual delineation by experts is still common practice for high quality segmentation, it is time-consuming and subjective. Neuroimaging studies tend to become ever larger and manual segmentation with its time needs and low reproducibility is ill-suited for such large imaging studies.

Email: martin_styner@ieee.org, WWW: www.ia.unc.edu

Many methods have been proposed in the literature for automatic/semi-automatic brain segmentation.[1] Deformable models, which deform a template based on the extracted image feature, have been employed in numerous medical imaging applications.[2] However these methods often rely on human experts for initialization and guidance. Ho et al. segment brain tumors using an automatic level-set snake evolution.[3] The construction of an atlas can help significantly in the segmentation. Leventon et al.[6] and Tsai et al.[7]use a shape-based approach to curve evolution for the segmentation of medical images containing known object types. Andreasen et al.[8] use a registration to the Talairach space where one brain has been manually segmented into subregions. Fischl et al.[4] use a fully, manually labeled atlas which is registered with a Bayesian approach to the image to segment. In[9] they proposed a biased atlas with probability maps for each subcortical structures. The atlas is then registered to each case along with the spatial priors. An hierarchical, atlas based expectation-Maximization segmentation algorithm[10] is used by Phol et al. As in this paper, some of the above mentioned researchers use atlases with spatial priors that are registered onto the studied brains. They differ from our method either by the atlas creation method or the employed registration technique.

In this paper we describe our automatic segmentation method employing an unbiased diffeomorphic atlas with probabilistic spatial priors built from a training set of MR images with corresponding manual segmentations. There are two main steps in our segmentation procedure: 1) Atlas creation with probabilistic spatial knowledge of the subcortical structures and 2) Registration of the atlas and the subcortical structure probabilistic maps to each case. Both steps employ a large deformation, fluid registration method developed by Joshi et al.[11] The atlas is created by a joint deformable registration of 10 training MRI datasets into a single unbiased average image. Along with the MRI registration, the manually segmented structures are deformed in the atlas coordinate space to create a probabilistic map. Once the atlas and the probabilistic maps are computed, we register the template image onto each case using an affine followed by a fluid registration. The computed deformation is then applied to the probabilistic maps of each structure and thresholded to form the segmentation. In the next section we describe this methodology in further detail and then present the set of validation and reliability studies performed in order to assess the performance of our method.

2. METHODS

In this section we describe our segmentation algorithm. Our approach is based on an unbiased diffeomorphic atlas with probabilistic spatial priors built from a training set of images with corresponding manual segmentations. Using the transformation fields from the previous step we generate probabilistic maps for each subcortical structure. When applying the atlas for automatic structural segmentation, each image is preprocessed with an intensity inhomogeneity correction, a skull stripping and an intensity calibration to the atlas. Then the atlas is registered to the image using an affine followed by a deformable registration matching the gray level intensities. Lastly, the registration transformations are applied to the probabilistic maps of each structure, which are then threshold at 0.5 probability. First we present the preprocessing steps needed for the registration/segmentation step. Second the atlas building process is described in more detail, and finally we explain the subcortical structure segmentation.

2.1. Image Preprocessing

As discussed further below in section 2.2, all images used in the atlas computation as well as the segmentation computation are initially preprocessed regarding image alignment and intensity calibration. The two preprocessing procedures are similar, differing only in regard to the initial alignment, which is applied to each image to be segmented. In this section we describe the four different steps of this preprocessing as illustrated in Figure 1.

The first preprocessing step registers each image to a prior digital atlas. During the atlas computation, an affine (15 parameters) registration to a separate fuzzy atlas was performed. The fuzzy atlas was generated from 155 normal adult subjects and is distributed with the SPM package. During the segmentation step, a rigid (6 parameters) registration to the unbiased average image generated in the atlas computation steps is performed. The employed registration software, provided by Daniel Rueckert,[12] is based on minimizing normalized mutual information and cubic spline intensity interpolation.

The second preprocessing step computes a brain tissue classification for all images using our itkEMS tool.[13–15] This tool computes a probabilistic atlas driven automatic tissue segmentation that employs the before mentioned

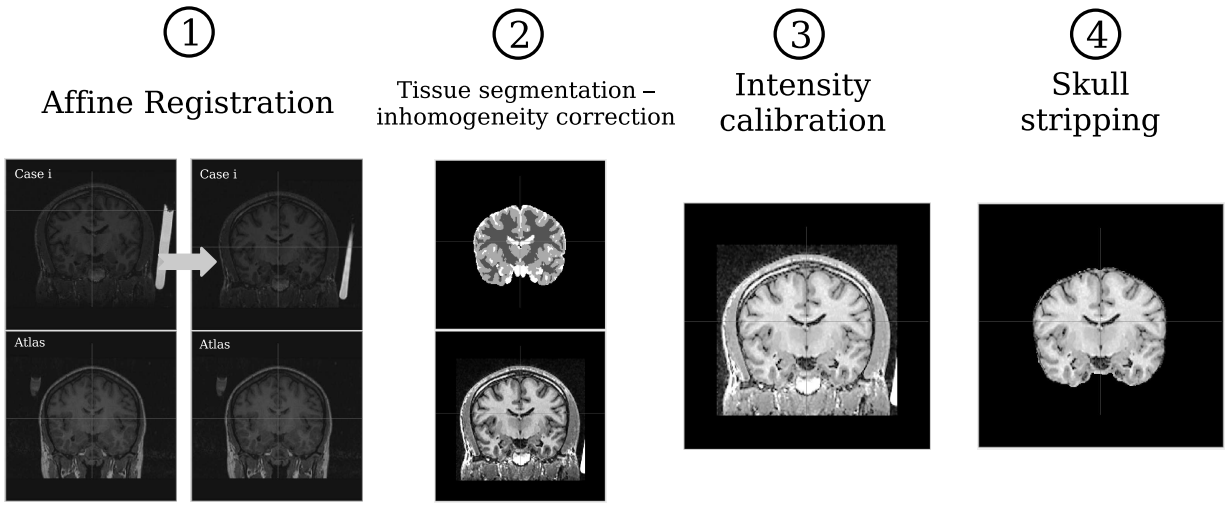

Figure 1. The four steps of our preprocessing procedure. First the image is affinely registered to the atlas. Then the tissue segmentation and the inhomogeneity correction are computed using our itkEMS software. The third step is the intensity calibration, and finally the image is skull stripped.

fuzzy SPM atlas. This tool further performs an intensity inhomogeneity correction of the image that removes gradual variations in the image intensities mainly due RF coil imperfections. The output consists of the corrected grayscale image along with binary and probabilistic maps of the tissue classes of white matter (WM), gray matter(GM), cerebrospinal fluid tissue(CSF).

In the next preprocessing step, the intensities of the images are calibrated. The deformable registration process that is central to both the atlas and segmentation computations, matches directly the image intensities. Thus an appropriate intensity calibration, additional to a prior intensity inhomogeneity correction, is crucial for the computation of a high quality average image and segmentation result. Our intensity calibration method normalizes all training images into the same intensity range via a spline based histogram transfer function that matches the mean intensities of the tissue classes of WM, GM and CSF, as well as the overall range of the image intensities. The mean tissue intensities are estimated using the probabilistic segmentation maps computed during the tissue classification from step 2.

As our interest is solely in segmenting brain regions, all images are skull stripped in the fourth and last step. The skull stripping also enhances the fidelity of the deformable registration process, as the most inferior axial slice often cuts the anatomical information at different levels and thus the differences of facial coverage would hamper the quality of the deformable registration. The skull stripping procedure was based on a mask generated from the binary tissue segmentation obtained in step 2. The mask is a fusion of the WM, GM and CSF area followed by a light mean curvature smoothing and a morphological opening operation filter. This operation defines the cutoff in the brain-stem region via the matched fuzzy atlas used in the tissue segmentation procedure.

After this preprocessing, all images are aligned in the same anatomical space, skull stripped, their intensity inhomogeneity is corrected and normalized. All of these steps are computed fully automatically via shell scripting. The resulting images are used as inputs in the atlas computation and the subcortical structure segmentation.

2.2. Atlas Computation

As a central step of our method, we build an atlas consisting of the average image and the corresponding spatial probabilistic maps of the subcortical structures from a given training image population, which had been already segmented (see Figure 2). The main step for our atlas computation is the diffeomorphic, non-rigid registration of each training image to an iteratively updated unbiased average image[11] that has minimal deformation to all training images. Using the deformable registration information, the segmentations are mapped into the average image space for the computation of the probabilistic maps.

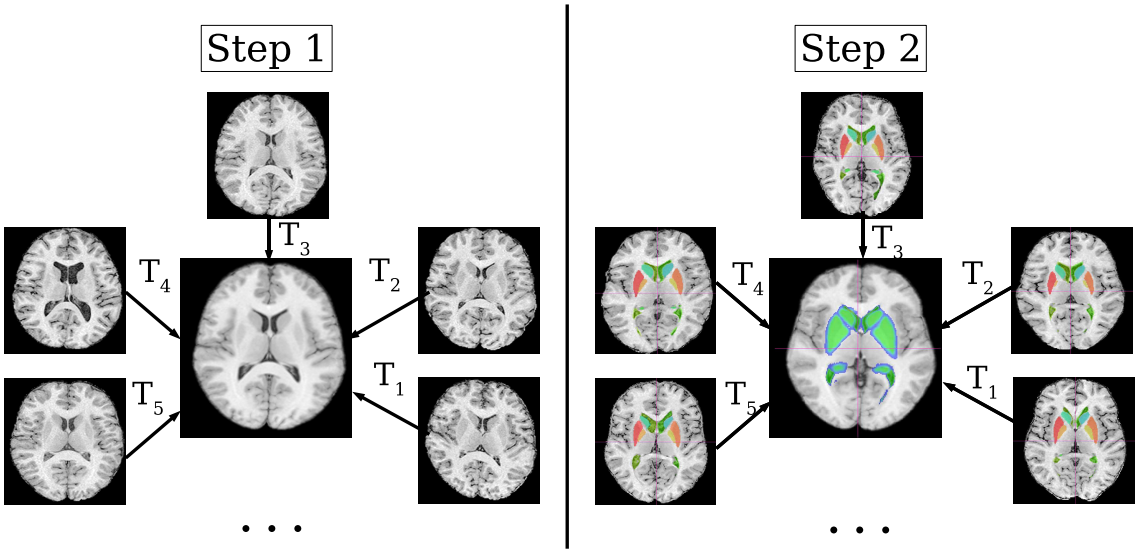

Figure 2. During the atlas creation process, structural images are averaged via a diffeomorphic, non rigid registration to an iteratively updated unbiased average image. Once the transformations are computed they are applied to the probabilistic maps of each structure (here the ROIs are gathered on the same image for display purpose but in our procedure each structural map is a separate probabilistic image).

As the studies in our laboratories deal with early pediatric as well as adult human data, we computed separate atlases for both populations. Complete subcortical structure segmentations of hippocampus, amygdala, putamen, globus pallidus, caudate and lateral ventricle (on both hemispheres) were only available for pediatric datasets, and thus we first computed the atlas image and probabilistic maps for the pediatric population. Then the atlas image for the adult cases were computed and the probabilistic maps of the pediatric atlas were mapped from the pediatric average image to the adult average image.

The pediatric atlas was created from a dataset of 10 subjects at ages 2 and 4 years, totaling in 20 training datasets of high resolution IR-prepped SPGR (T1-weighted, GE 1.5T) MR images.[16,17] For each of these 20 training datasets the subcortical structures have been segmented by experts* either via manual outlining, or semi-automatic geodesic curve evolution.[18]

After the preprocessing step (see section 2.1), we use deformable registration to compute the unbiased average image[11] from the whole training population, along with deformation fields containing the information to transform each image to the atlas (see Figure 2). The deformable registration refines iteratively a mean average and computes a fluid-model based deformation field via voxel-by-voxel diffeomorphic mapping to that average image.

*See this link `http://www.psychiatry.unc.edu/autismresearch/mri/roiprotocols.htm` for a detailed description of protocols and reliability results.

The registrations (affine and deformable) are applied to the prior structural segmentations for each training case in order to create the probabilistic map of the subcortical structures via averaging.

We applied the same processing as for the pediatric atlas to a training population of adult cases in order to compute a separate adult atlas. The images of 10 healthy adult control subjects (20 to 55 year old, IR-prepped SPGR, GE 1.5) were selected, preprocessed and their unbiased average image was generated via our atlas computation procedure. In our experience, despite the difference in head size from pediatric cases at age 4 to adult cases, the sub cortical structures of a pediatric brain are quite similarly shaped to those of an adults. We thus adapted the pediatric structural probabilistic maps to the adult atlas via affine followed by non-rigid diffeomorphic registration of the pediatric atlas image to the adult atlas image. These transformations were then applied to the subcortical probabilistic maps of the pediatric atlas to yield the spatial probabilistic maps of the adult atlas.

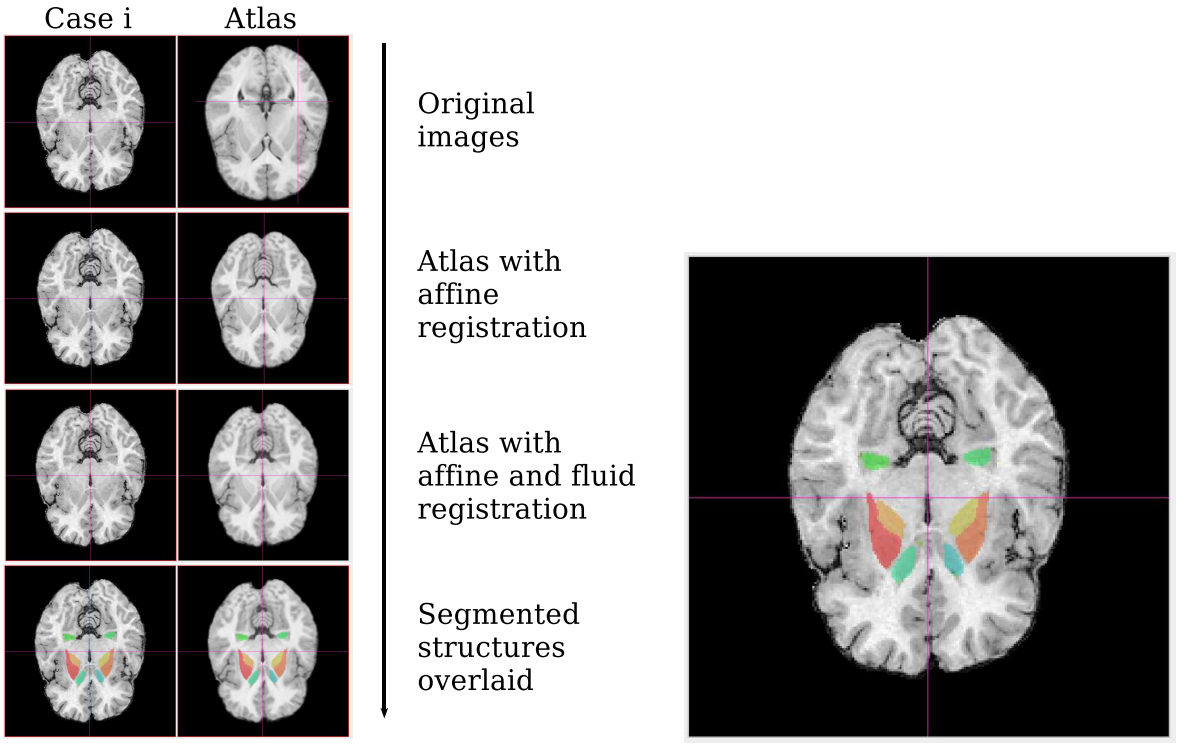

(a) Segmentation procedure

(b) Final ROIs

Figure 3. Description of the segmentation procedure. (a) The main steps of the registration. Top:original atlas image alongside the case image, 2nd row: atlas affinely registered to the case, 3rd row: atlas registered with the fluid deformation, 4th row: final image with the ROIs overlaid. (b) The ROIs of a selected case.

2.3. Atlas based Segmentation

In this section we describe the subcortical structure segmentation process (see Figure 3). By mapping the atlas template image with its probabilistic structural definitions to the preprocessed images (aligned, intensity inhomogeneity corrected, intensity calibrated, skull stripped) we compute the subcortical structure segmentation.

The segmentation process starts by mapping the atlas image onto the current T1 image using a two step registration process. First, we used an affine registration with 15 parameters (translation, rotation, scaling and

skew) to place the atlas image roughly in the current case image coordinate frame. After the application of the affine transformation, the large scale brain information is aligned but the affine registration cannot match the finer scale brain variations. Second, the affinely registered atlas image is further registered to the current image using the same fluid, diffeomophic, deformable registration process used for the atlas computation.

Both affine and deformable registration information are applied to map the probabilistic subcortical structural from the atlas space to the current image space. This results in a probabilistic map in the current patient's coordinate space for all the ROIs.

The final segmentation of all structures, with the exception of the lateral ventricles, are then computed by thresholding the probabilistic maps at 50% probability. The final volume is a binary image with a probability of the structure presence greater than 0.5. Due to the large variability of the lateral ventricles, we chose a different approach for the lateral ventricle segmentation. Instead of manipulating a probabilistic map of the lateral ventricles in the atlas template space, we use a binary mask applied to the prior CSF tissue segmentation. This binary mask in the atlas space is computed by thresholding the ventricle probabilistic map at 0.5, followed by a dilation. The transformed (affine and fluid) mask is then applied to the CSF probabilistic map generated by the itkEMS tool. This last step creates a probabilistic map of the lateral ventricles for each subject, which in turn is thresholded at 0.5.

3. RESULTS

Once the atlas is created, the subcortical structure segmentation takes less than 2 hours on a regular PC (Intel Xeon processor 2.4 GHz). Thus we have been able to apply our procedure on several datasets in order to validate the segmentation procedure. In this section we describe, first, the reproducibility of our method and then the agreement with manual segmentations.

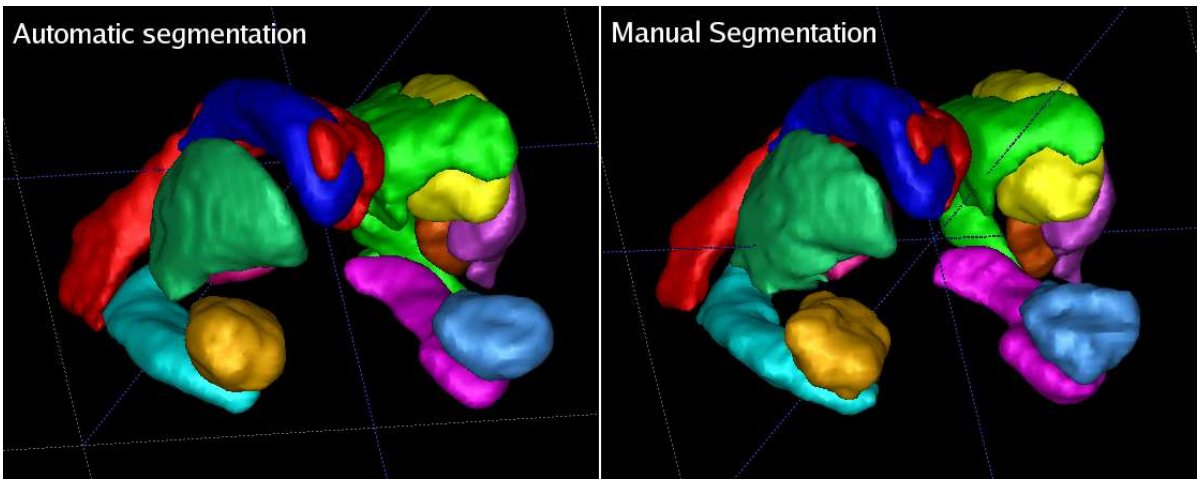

Figure 4. Segmentation comparisons between manually segmented structures and the structures segmented by our procedure in a healthy adult case.

3.1. Reproducibility/Repeatability

One of the main test for the validity of a segmentation method is the reproducibility. The main purpose of this test is to know if similar cases are segmented in similar ways. As single adult subject (age 28) has been scanned ten times on five different scanners (4 GE 1.5 Tesla, 1 Phillips 1.5 Tesla scanner) within 6 weeks.[14] Each of these scans was segmented with our method. We were interested in how different each structure was from the other scan structures, assuming that the brain morphometry stayed stable. We computed the mean volume of

the structure probabilistic maps for each case. Then the coefficient of variance (average volume divided by the standard deviation) describes how close the volumes are to each other.

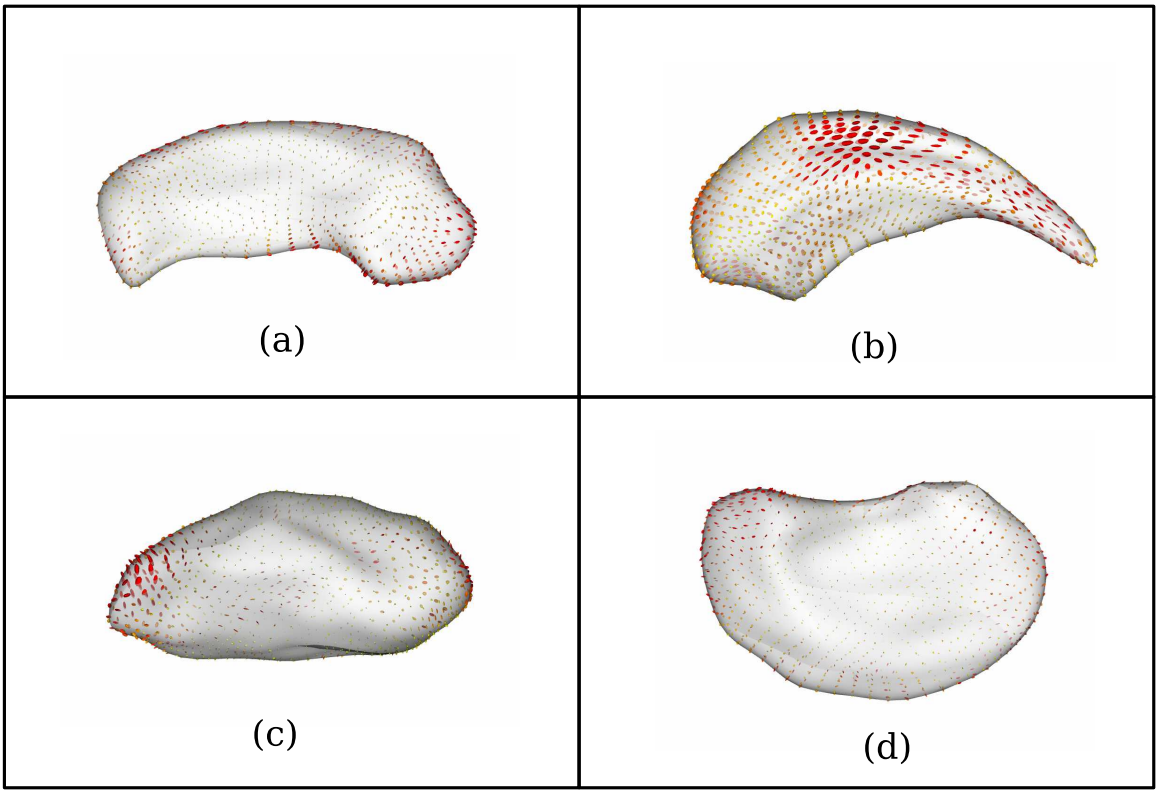

Figure 5. Variability/Error ellipsoid for four structures ((a) Hyppocampus (b) Caudate (c) Pallidus (d) Putamen) over both hemispheric structures in 10 scans of the same person in the reliability study (from selected viewing angles). No additional shape base alignment was performed and thus the variability contains both registration (from the preprocessing step) and segmentation differences. The ellipsoid axes magnitude represents the standard deviation along each axis.

As one can see in Table 1, the coefficient of variances are quite small for all structures. Except for the lateral ventricles the structures are segmented with less than a 1% difference of their total volume. These results show an excellent repeatability for our segmentation, which are a factor 5-7 smaller than manual segmentations reported in.[14] Thus, not entirely surprising, our automatic method is more reliable and more efficient than manual segmentations.

In order to get a visual assessment of the local reproducibility of our method, we additionally computed for each structure the average local shape variability of the 10 images. This variability was computed on the raw segmentations without additional shape based registration (such as rigid Procrustes alignment). The resulting variability thus represents both registration as well as segmentation errors. As shown in Figure 5 the variation of each structure away from the average shape are rather small. Furthermore, the maximal surface standard deviation is lower than half a voxelsize of the original images for all structures except the lateral ventricle.

3.2. Validation to Human Expert Segmentations

Once the reproducibility of our method is validated, the next step is to compare our automatically segmented structures to the manually segmented ones. We use several indicators to assess our segmentation: the intraclass correlation coefficient (ICC), which quantify the inter-rater accuracy of volumetric measurements, the Pearson

Table 1. Coefficients of variance (average volume divided by the standard deviation) of all structural volumes for the ten scans of the same subjects. L= Left, R = Right hemispheric structure.

Structure (Left & Right)	Coefficient of variance(%)
Amygdala L	0.75
Amygdala R	0.66
Caudate L	0.78
Caudate R	0.43
Hippocampus L	0.91
Hippocampus R	1.02
Lat Ventricle L	2.34
Lat Ventricle R	1.45
Pallidus L	0.57
Pallidus R	0.70
Putamen L	0.43
Putamen R	0.63

correlation coefficient, which measures the correlation of the volumetric measurements across subjects and methods, as well as the dice coefficient, which incorporate the actual shape of the segmentation into the validity assessment of the local shape structures. The dice coefficient is computed as the volume of the union of the structures divided by their average volume. The ICC measures are not as well suited as the Pearson correlation coefficients in our tests as no intra-subject variation can be measured (no manual repetition of the segmentations, and automatic method has no intra-subject variation as it is a deterministic computation).

These validation measurements have been computed on two different studies. The first one is the Internet Brain Segmentation Repository (IBSR) v2.0, which is an open online database with 18 MR brain 3D images and their associated segmentations[†]. These consist of high resolution T1 weighted MRI images acquired with a similar imaging protocol as the one used in our training population. The second study consists of further datasets from an autism study already described in 2.2. The training and testing dataset are mutually exclusive, both sets include control and autistic subjects at age 2 and 4 years.

Table 2. ICC and correlation coefficients for the IBSR and the autism dataset. The ICC measures are not as well suited as the correlation coefficients as no intra-subject variation can be measured.

Dataset	IBSR		Autism	
Structure (Left & Right)	ICC	Correlation	ICC	Correlation
Ventricle L	0.923	0.97	0.601	0.98
Ventricle R	0.935	0.98	0.584	0.98
Caudate L	0.748	0.86	0.707	0.75
Caudate R	0.881	0.93	0.663	0.72
Hippocampus L	0.089	0.8	-0.007	0.18
Hippocampus R	0.241	0.74	0.055	0.16
Amygdala L	-0.140	0.42	0.333	0.44
Amygdala R	-0.210	0.42	0.500	0.53
Putamen L	0.770	0.9	0.759	0.78
Putamen R	0.810	0.9	0.819	0.84
Pallidus L	0.807	0.82	0.487	0.56
Pallidus R	0.845	0.86	0.504	0.77

[†]Available at `http://www.cma.mgh.harvard.edu/ibsr/` The Internet Brain Segmentation Repository (IBSR).

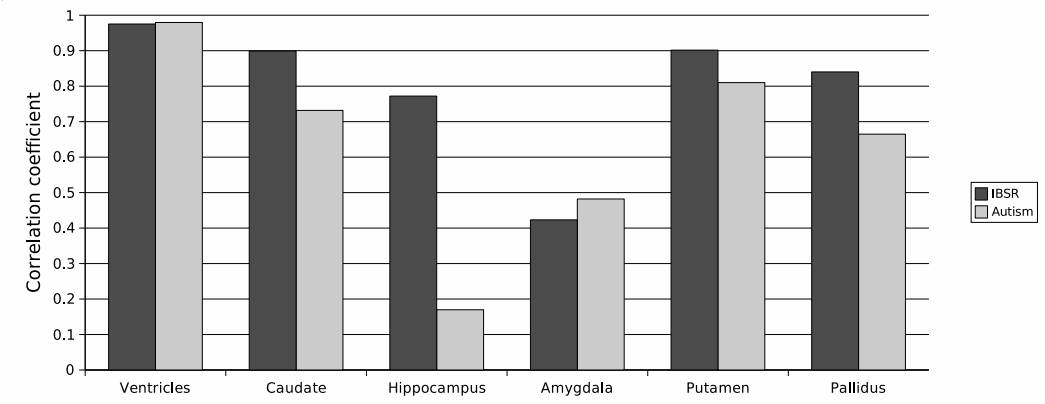

Figure 6. Structure average correlation coefficients for the IBSR and the autism dataset

The results in Figure 6 and Table 2 show that the ventricles, the caudates, the putamen and the pallidus have a high intra-rater reliability, especially considering the Pearson correlation coefficient. For the hyppocampy and the amygdala, the Pearson correlation are appropriate for the adult IBSR study, but are not fully satisfactory in the pediatric autism study.

The next indicator used to validate our method is the dice coefficient quantifying the volume overlap. The dice coefficients averaged by structures are displayed in Figure 7. We can see that for the Autism group, all the structures, except the ventricles because of their wide variation range, present a value above 70%. For the IBSR data, the values are smaller but still around 70%. These results show a good matching for all structures. The lower dice coefficients in the IBSR study is likely due to different definitions of the segmentation protocol.

Overall, the different validation measures show a mixed picture. The basal ganglia (caudate, putamen and globus pallidus) show good validation for all measures, but the amygdala and hippocampus show only intermediate correlation coefficients, but nevertheless good dice coefficients.

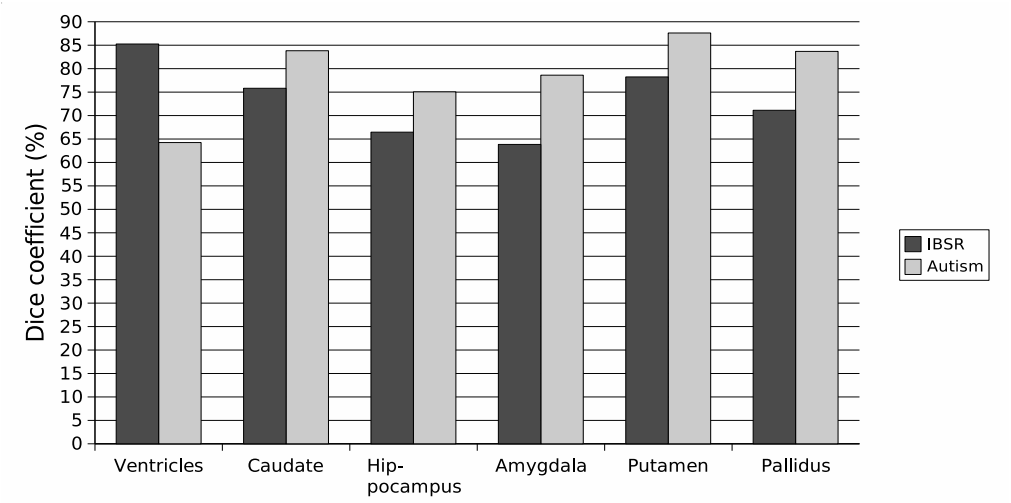

Figure 7. Structure average dice coefficient for the IBSR and the autism dataset

4. CONCLUSIONS AND DISCUSSION

A new segmentation scheme employing registration of a template atlas image with probabilistic structural priors has been presented. The atlas is created through an unbiased, diffeomorphic procedure from manually segmented structures. The probabilistic maps in the atlas coordinate frame are mapped on the cases with transformations (affine and fluid) from the registration of the atlas to the current case.

The segmentation builds on a series of existing software tools. The tissue segmentation performed with the itkEMS tool,[13–15] the affine registration using D. Rueckert RView program,[12] the unbiased diffeomorphic atlas creation using S. Joshi's tool[11] are combined here to perform our segmentation.

Our thorough validation shows that the basal ganglia can be segmented both accurately and reliably. Also the hippocampus and amygdala segmentation are reliable, but the comparison to manual segmentation is rather mixed, but still satisfying. The lateral ventricles are also well segmented, albeit with a bit lower reliability than all the other structures.

Even though our results suggest the appropriateness of our method, manual segmentation is still the gold standard. However, this fully automatic pipeline allows the efficient and reliable processing of large scale studies. We recently applied this method to a study with over 800 datasets. The whole computation and quality control process took less than 2 weeks, but several man-years of work would have been necessary for manual expert segmentations.

The proposed methodology is sensitive to the quality of the non-rigid registration of the atlas template to each case. We have not observed any full failure in any of our tests, but for a small subset of our data (less than 1%), individual segmentations had to be rejected.

Our segmentation is further dependent on the choice of the atlas dataset. We observed that the closer the characteristics (MRI scanner type, imaging protocol, subject population) of the segmented image the better the segmentation quality. The preprocessing steps aim at reducing that atlas bias, but it is obviously impossible to fully remove this bias in an atlas based segmentation method.

ACKNOWLEDGMENTS

We would like thank Daniel Rueckert for the rigid and affine registration tool used in this paper. Matthieu Jomier has also contributed software developments in several of the segmentation steps. We further want to thank Cecile Charles and the Duke Image Analysis Laboratory for providing access to the Quality Control study. This research has been supported by the UNC Neurodevelopmental Disorders Research Center HD 03110 (J. Piven). We acknowledge also the support from Lilly Eli with a user initiated information technology grant (PCG TR:033107).

REFERENCES

1. D. Pham, C. Xu, and J. Prince, "Current methods in medical image segmentation," *Annu Rev Biomed Eng* **2**, pp. 315–337, 2000.
2. M. Sonka and J. Fitzpatrick in *Handbook of medical imaging. Med. Image Process. Anal., SPIE Press*, **1 and 2**, pp. 69–211, 2000.
3. S. Ho, E. Bullitt, and G. Gerig, "Level set evolution with region competition: Automatic 3-d segmentation of brain tumorslclasslation," *International Conference on Pattern Recognition* , pp. 532–535, August 2002.
4. B. Fischl, D. Salat, E. Busa, M. Albert, M. Dieterich, C. Haselgrove, A. van der Kouwe, R. Killiany, D. Kennedy, S. Klaveness, A. Montillo, N. Makris, B. Rosen, and A. Dale, "Whole brain segmentation: automated labeling of neuroanatomical structures in the human brain," in *Neuron*, **33**, pp. 341–355, January 2002.
5. A. Kelemen, G. Székely, and G. Gerig, "Elastic model-based segmentation of 3d neuroradiological data sets," *IEEE Trans. Med. Imaging* **18**, pp. 828–839, October 1999.
6. M. Leventon, W. Grimson, and O. Faugeras, "Statistical shape influence in geodesic active contours," in *IEEE CVPR*, **1**, pp. 316–323, 2000.

7. A. Tsai, A. Yezzi, W. Wells, C. Tempany, D. Tucker, A. Fan, W. Grimson, , and A. Willsky, "A shape-based approach to the segmentation of medical imagery using level sets," *IEEE Transactions on Medical Imaging* **22**(2), pp. 137–154, 2003.
8. N. Andreasen, R. Rajarethinam, T. Cizadlo, S. Arndt, V. n. Swayze, L. Flashman, D. O'Leary, J. Ehrhardt, and W. Yuh, "Automatic atlas-based volume estimation of human brain regions from mr images," *Journal of Computer Assisted Tomography* , pp. 98–106, 1996.
9. J. Zhou and J. C. Rajapakse, "Segmentation of subcortical brain structures using fuzzy templates," *NeuroImage* **28**, pp. 915–924, December 2005.
10. K. Pohl, S. Bouix, R. Kikinis, and W. Grimson, "Anatomical guided segmentation with non-stationary tissue class distributions in an expectation-maximization framework," in *ISBI 2004*, pp. pp. 81–84, IEEE International Symposium on Biomedical Imaging: From Nano to Macro, 2004.
11. S. Joshi, B. Davis, M. Jomier, and G. Gerig, "Unbiased diffeomorphic atlas construction for computational anatomy," *NeuroImage* **23**, pp. S151–S160, 2004.
12. D. Rueckert, L. Sonoda, C. Hayes, D. Hill, M. Leach, and D. Hawkes, "Nonrigid registration using free-form deformations: application tobreast mr images," *IEEE Transactions on Medical Imaging* **18**(8), pp. 712–721, 1999.
13. K. Van Leemput, F. Maes, D. Vandermeulen, and P. Suetens, "Automated model based tissue classification of mr images of the brain," *IEEE Transactions on Medical Imaging* **18**(10), pp. 897–906, 1999.
14. M. Styner, H. C. Charles, J. Park, J. Lieberman, and G. Gerig, "Multi-site validation of image analysis methods - assessing intra and inter-site variability," in *SPIE Medical Imaging*, *Proc. SPIE* **4684**, pp. 278–286, 2002.
15. M. Prastawa, J. H. Gilmore, W. Lin, and G. Gerig, "Automatic segmentation of mr images of the developing newborn brain," *Medical Image Analysis* **9**, pp. 457–466, October 2005.
16. H. C. Hazlett, M. D. Poe, G. Gerig, R. G. Smith, and J. Piven, "Cortical gray and white brain tissue volume in adolescents and adults with autism," *Biological Psychiatry* **59**, pp. 1–96, January 2006.
17. J. Piven, S. Arndt, J. Bailey, and N. Andreasen, "Regional brain enlargement in autism: a magnetic resonance imaging study," *Journal Of The American Academy Of Child And Adolescent Psychiatry* **35**, pp. 530–536, April 1996.
18. P. Yushkevich, J. Piven, H. Cody Hazlett, R. Gimpel Smith, S. Ho, J. Gee, and G. Gerig, "User-guided 3d active contour segmentation of anatomical structures: Significantly improved efficiency and reliability," *NeuroImage* **31**, pp. 1116 – 1128, 2006.